Novel Method to Study Neutron Capture of ^{235}U and ^{238}U Simultaneously at keV Energies

A. Wallner,[1,2,*] T. Belgya,[3] M. Bichler,[4] K. Buczak,[2,4] I. Dillmann,[5,6] F. Käppeler,[5] C. Lederer,[2,7,†] A. Mengoni,[8] F. Quinto,[2,‡] P. Steier,[2] and L. Szentmiklosi[3]

[1]*Department of Nuclear Physics, RSPE, Australian National University, Canberra, Australian Capital Territory 0200, Australia*
[2]*Faculty of Physics, VERA, Isotope Research & Nuclear Physics, University of Vienna, 1090 Vienna, Austria*
[3]*Nuclear Analysis and Radiography Department (NARD), Centre for Energy Research, Hungarian Academy of Sciences, 1525 Budapest, Hungary*
[4]*Atominstitut, Vienna University of Technology, 1040 Vienna, Austria*
[5]*Institut für Kernphysik, Karlsruhe Institute of Technology (KIT), Campus North, 76021 Karlsruhe, Germany*
[6]*TRIUMF, Vancouver, British Columbia V6T2A3, Canada*
[7]*Institute for Applied Physics, Goethe University Frankfurt, 60438 Frankfurt, Germany*
[8]*Agenzia nazionale per le nuove tecnologie, l'energia e lo sviluppo economico sostenibile (ENEA), 40129 Bologna, Italy*

(Received 29 January 2014; published 14 May 2014)

The neutron capture cross sections of the main uranium isotopes, ^{235}U and ^{238}U, were measured simultaneously for keV energies, for the first time by combining activation technique and atom counting of the reaction products using accelerator mass spectrometry. New data, with a precision of 3%–5%, were obtained from mg-sized natural uranium samples for neutron energies with an equivalent Maxwell-Boltzmann distribution of $kT \sim 25$ keV and for a broad energy distribution peaking at 426 keV. The cross-section ratio of $^{235}\mathrm{U}(n,\gamma)/^{238}\mathrm{U}(n,\gamma)$ can be deduced in accelerator mass spectrometry directly from the atom ratio of the reaction products $^{236}\mathrm{U}/^{239}\mathrm{U}$, independent of any fluence normalization. Our results confirm the values at the lower band of existing data. They serve as important anchor points to resolve present discrepancies in nuclear data libraries as well as for the normalization of cross-section data used in the nuclear astrophysics community for s-process studies.

DOI: 10.1103/PhysRevLett.112.192501 PACS numbers: 25.40.Lw, 07.75.+h, 28.41.Ak

Highly accurate nuclear data for minor actinides and the main fuel materials (U, Pu) are the primary nuclear ingredient for the design of advanced reactor concepts. Neutron capture cross sections for ^{235}U and ^{238}U are well known for thermal energies, but data in the keV to MeV energy range show significant discrepancies, mainly due to the lack of high intensity and well-characterized neutron sources, and difficulties with measurements of the neutron fluence. Existing data for the capture channel are based on time-of-flight (TOF) techniques [1–3] and also on activation in the case of ^{238}U. A major difficulty in these experiments is the discrimination against the γ background from the strongly competing fission channel. Discrepancies in experimental data and data libraries indicate that previous measurements might have suffered from multiple scattering corrections, because large sample masses were required. Moreover, recent studies [4,5] exhibit significant differences in the (n,γ) cross sections of ^{235}U and ^{238}U at keV energies between major nuclear-data libraries [4–8]; in particular, for ^{235}U recent results suggest discrepancies of 25% near 1 keV [4,5]. Therefore, remeasurements of these reactions are recommended in the Nuclear Energy Agency high priority request list [9]. A fair number of experimental data are published for $^{238}\mathrm{U}(n,\gamma)$ [10] (see Supplemental Material [11]), however, only two new data sets exist for $^{235}\mathrm{U}(n,\gamma)$ in the keV energy range [1,12] since 1980 (Supplemental Material, Fig. S1 [11]). Recently, Jandel *et al.* [1] reported precision TOF measurements for $^{235}\mathrm{U}(n,\gamma)$ obtained with the DANCE setup at Los Alamos for energies between 1 eV and 1 MeV with uncertainties of 2%–3% below 1 keV, and of 8% and 20% for 25 and 500 keV, respectively.

In this work we applied a novel and independent technique to existing methods by combining neutron activation with subsequent atom counting using accelerator mass spectrometry (AMS). This offline counting method of the reaction products is complementary to TOF measurements. AMS provides data with a precision as high as 0.2% (radiocarbon dating) and typically of a few percent for actinides [13–17], completely free of interference with fission or any other background. Because radionuclides are measured in AMS with by far the highest sensitivity via isotope ratios, sample masses between a few and some tens of mg are sufficient. The conversion ratio in a nuclear reaction is only a function of the particle (neutron) fluence and the cross section Eq. (1), independent of the sample mass and, due to the low masses used, not affected by multiple-scattering corrections. AMS is suited for cross-section studies at single energy points or in well-defined neutron spectra rather than providing detailed cross-section data over a wide energy range. Accordingly, AMS can provide accurate anchor points for critical reactions leading to radioactive nuclides for specific energies with the important aspect of being fully complementary and independent of previous experiments [17,18]. This work is also

important for nuclear astrophysics since it relates to the fluence normalization for a range of neutron cross-section measurements relevant to *s*-process nucleosynthesis (see below) and, in addition, this method, utilizing identical irradiation setups, is being used as an important extension for s-process neutron-capture studies [19–22].

We have applied this approach to a simultaneous measurement of the (n, γ) cross sections of ^{235}U and ^{238}U in the keV energy range. According to the reaction scheme sketched in Fig. 1, neutron capture on ^{235}U produces long-lived ^{236}U ($t_{1/2} = 23.4$ Myr), and the cross section was determined directly by the isotope ratio $^{236}\mathrm{U}/^{235}\mathrm{U}$ measured via AMS and the neutron fluence Φ_E,

$$\sigma_E(n,\gamma) = \frac{^{236}\mathrm{U}}{^{235}\mathrm{U}}\frac{1}{\Phi_E}. \quad (1)$$

The fluence was determined from gold foils simultaneously irradiated with uranium. Neutron capture on ^{238}U forms ^{239}U, which decays via ^{239}Np to long-lived ^{239}Pu (24.1 kyr). The cross-section ratio of ^{235}U and ^{238}U capture can also be expressed by the isotope ratio of the reaction products and the natural abundance of ^{235}U and ^{238}U, completely independent of the neutron fluence. This ratio is therefore only dependent on the AMS data (and a well-known spike of ^{242}Pu which serves as a reference for AMS, see below). After an appropriate waiting time, ^{239}U decays completely to ^{239}Pu. Thus Eq. (2) consists of two AMS isotope-ratios ($^{239}\mathrm{Pu}/^{242}\mathrm{Pu}$, $^{236}\mathrm{U}/^{238}\mathrm{U}$) as well as the natural $^{235}\mathrm{U}/^{238}\mathrm{U}$ ratio, the spike ^{242}Pu and the number of ^{238}U atoms.

$$\frac{\sigma_{\mathrm{U}-8(n,\gamma)}}{\sigma_{\mathrm{U}-5(n,\gamma)}} = \frac{^{239}\mathrm{U}}{^{238}\mathrm{U}} \Big/ \frac{^{236}\mathrm{U}}{^{235}\mathrm{U}} = \frac{^{239}\mathrm{U}}{^{236}\mathrm{U}}\frac{^{235}\mathrm{U}}{^{238}\mathrm{U}} = \frac{^{239}\mathrm{Pu}}{^{242}\mathrm{Pu}}\frac{^{238}\mathrm{U}}{^{236}\mathrm{U}}\frac{^{235}\mathrm{U}}{^{238}\mathrm{U}}\frac{^{242}\mathrm{Pu}}{^{238}\mathrm{U}}. \quad (2)$$

The number of ^{238}U atoms can be calculated from the sample mass. However, this number depends on the stoichiometry, and uranium oxide can be either in the form of U_3O_8 or U_2O_3 or any mixture. Thus, to verify the stoichiometry we compared the measured AMS ratios ($^{239}\mathrm{Pu}/^{242}\mathrm{Pu} \times ^{242}\mathrm{Pu}/^{238}\mathrm{U}$) of samples irradiated with thermal neutrons, with the ratio calculated from the well-known thermal $^{238}\mathrm{U}(n,\gamma)$ cross-section value (see below). Further, we added simultaneously with the ^{242}Pu spike a well-known amount of ^{233}U as an additional reference for ^{236}U counting.

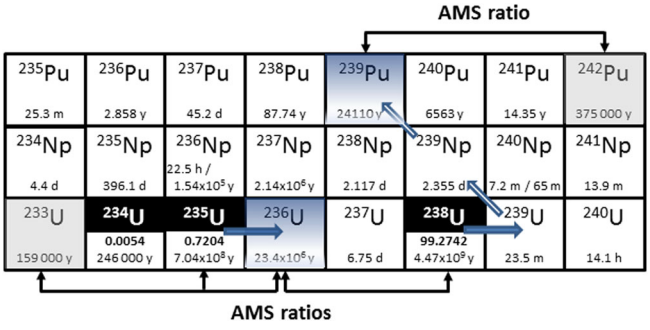

FIG. 1 (color online). Chart of the nuclides: long-lived neutron-capture products selected for detection via AMS are ^{236}U ($t_{1/2} = 23.4$ Myr) and ^{239}Pu (24.1 kyr). A spike reference ^{233}U (159 kyr) and ^{242}Pu (375 kyr) [12] was added for $^{236}\mathrm{U}/^{233}\mathrm{U}$ and $^{239}\mathrm{Pu}/^{242}\mathrm{Pu}$ AMS measurements. ^{236}U was also measured relative to ^{235}U and ^{238}U.

Uranium-oxide powder with a natural ratio $^{238}\mathrm{U}/^{235}\mathrm{U} = 137.8$ was kindly provided by IRMM (material BC02061) [23]. Prior to the activations it was verified by AMS that the material contained low levels of ^{236}U [$^{236}\mathrm{U}/^{238}\mathrm{U} = (0.79 \pm 0.01) \times 10^{-11}$] and ^{239}Pu ($^{239}\mathrm{Pu}/^{238}\mathrm{U} < 5 \times 10^{-13}$). Pellets, 6 mm in diameter and ~0.2 mm thickness, were pressed; two for activations at keV energies at Karlsruhe Institute of Technology (KIT) [24] and two for irradiations with a beam of cold neutrons at the Budapest Neutron Centre (BNC) [25]. In all irradiations the uranium pellets were sandwiched by thin Au foils of the same geometry. At BNC, in addition, high-purity Au powder of 2.6 and 4.7 mg was homogeneously mixed into the uranium-oxide powder, forming a stack of Au-foil–(U/Au)-pellet–Au-foil, where the Au powder served as an additional monitor for probing the neutron beam profile.

At BNC, utilizing the 10-MW research reactor [26], two samples were irradiated over a period of about 5 and 8 d, respectively (Table I). The equivalent thermal neutron fluence was determined from decay measurements on ^{198}Au produced in the gold monitors. Because of the $1/v$ energy dependence of the capture cross section, the reaction rate scales exactly in the same way from cold to thermal energies for both gold and uranium, with the advantage that any interferences from resonances in the eV energy region are excluded at subthermal energies. The fluence values obtained from the Au foils and the Au powder gave consistent values within 1%.

Two uranium pellets were irradiated at the Karlsruhe 3.7-MV Van de Graaff accelerator with keV neutrons produced via the $^{7}\mathrm{Li}(p,n)$ reaction by bombarding a Li target with an intense proton beam of 80–100 μA at energies of $E_p = 1912$ and 2285 keV, respectively. Sample IRMM-a was irradiated with a quasistellar neutron energy distribution (Fig. 2). This setup was developed at Karlsruhe Institute of Technology (KIT) [27] and used over many years for identical irradiations to establish a comprehensive set of neutron-capture cross sections relevant for *s*-process nucleosynthesis [28]. With the neutron-energy distribution obtained in these irradiations ($E_p = 1912$ keV), the integrated cross section is best approximated with a Maxwell-Boltzmann averaged cross section (MACS) at an effective temperature of $kT = 25.3$ keV [27]. The neutrons were emitted in a forward cone and hit the uranium sample at a distance of 1.9 mm. The second pellet was irradiated at 2.9 mm distance with a broad neutron spectrum and a mean energy of 426 keV (Fig. 2).

TABLE I. Four uranium-oxide pellets (material IRMM BC0206-1), 6 mm in diameter, were used for neutron activations at KIT and BNC. All pellets were sandwiched by Au foils as neutron fluence monitors. The BNC fluence data are the thermal equivalent values.

Sample	Sample mass	Neutron irradiation	Neutron source	Neutron energy	Fluence (10^{14} cm^{-2})
IRMM-a	50.0 mg	KIT	^{7}Li(p,n)	$kT \sim 25$ keV	16.48 ± 0.38
IRMM-b	57.1 mg	KIT	^{7}Li(p,n)	426 keV	42.44 ± 1.02
IRMM-3	45.9 mg	BNC	Reactor	Cold/thermal	0.715 ± 0.016
IRMM-5	40.9 mg	BNC	Reactor	Cold/thermal	2.78 ± 0.06

An open geometry (the next wall was 3 m from the sample located) and a low-mass sample holder ensured that any influence from backscattered neutrons was negligible. Both experimental spectra were simulated with the code PINO [29] and used for the determination of the spectrum-averaged neutron-capture cross section (SACS) of ^{197}Au, ^{235}U, and ^{238}U (Table II). The total irradiation times for the 25 and 426 keV samples were 7 and 12 d, respectively, resulting in a fluence of 1.65×10^{15} and 4.24×10^{15} neutrons/cm^2 ($\pm 2\%$) [27,30] based on the spectrum-averaged ENDF/B-VII.1 Au cross section (623.0 and 157.8 mbarn) [4] (Table I and Supplemental Material, Table T1 [11]).

After the activations the four irradiated samples were split into independent fractions for chemical separation of ^{239}Pu (decay product of ^{239}U) from the uranium bulk material. These fractions were dissolved in nitric acid and a well-known amount of a certified ^{233}U-(IRMM-058), as well as of a certified ^{242}Pu-spike reference material (IRMM-085) [31] was added for quantitative tracing of the uranium and plutonium separation. The isotope ratios ^{236}U/^{233}U, ^{236}U/^{235}U, and ^{239}Pu/^{242}Pu, established at the start of sample chemistry remain constant, independent of the total chemical yield obtained in the process of sample preparation.

The plutonium and uranium fractions were separated via chromatographic columns based on TEVA® resin. First, the bulk uranium (several mg) was eluted and in a subsequent step Pu ($\sim 10^8$–10^{10} atoms) passed through the columns. An iron standard solution ($\sim$2 mg Fe) was added for iron-hydroxide coprecipitation of U and Pu. Finally, U/Pu oxides were produced in a matrix of iron oxide. A few mg of this material, mixed with Ag powder, was pressed into sample holders for AMS. About 30 AMS samples per pellet were available for the ^{236}U measurements. The Pu/Fe/Ag mixture was pressed into 7–10 sample holders per pellet.

The AMS measurements were performed at the Vienna environmental research accelerator (VERA) laboratory at the University of Vienna [13,17,32]. Negative uranium (plutonium)-oxide ions were extracted from the ion source, energy and mass analyzed and injected into a tandem accelerator. The tandem was typically operated at 3.0 MV terminal voltage. The negative ions were completely fragmented by an oxygen gas stripper in the terminal of the tandem thus eliminating any molecules present in the primary beam. In addition, electrons were stripped off the ions in the stripper, resulting in dominantly positive charge states, which were further accelerated in the second part of the tandem. From the transmitted beam, ions of charge-state

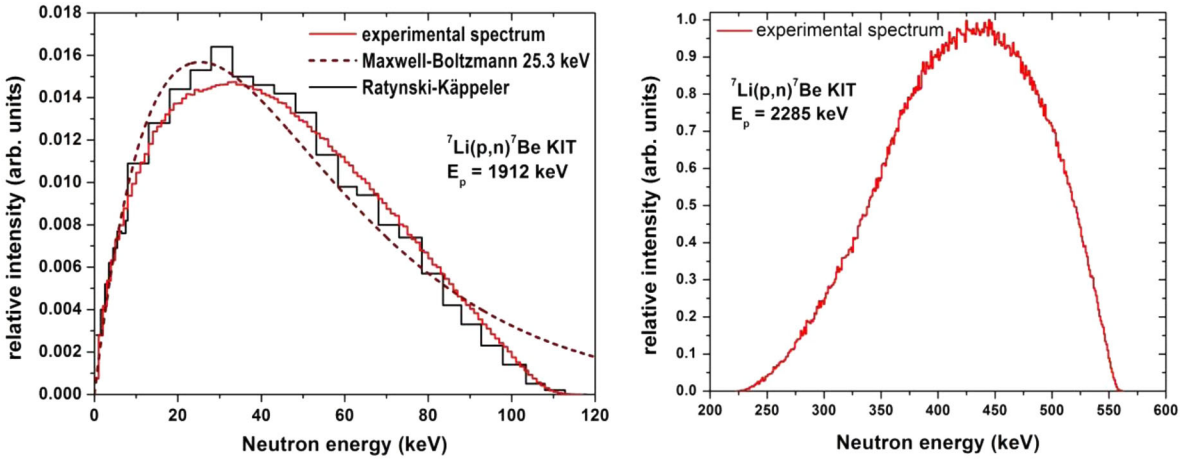

FIG. 2 (color online). Left: Experimental energy distribution (solid line, PINO [29]) which approximates a Maxwell-Boltzmann distribution of $kT \sim 25$ keV (dashed line). For comparison the measured quasistellar Ratynski-Käppeler spectrum [27] used for nuclear astrophysics studies is plotted as a histogram; right: energy distribution calculated with PINO for the neutron irradiation with $E_p = 2285$ keV.

TABLE II. a: Measured isotope ratios and final spectrum-averaged cross-section data for $^{235}U(n,\gamma)^{236}U$ compared to spectrum-averaged data given in data libraries. A 1.6% normalization factor was applied to IRMM-a and IRMM-b to reproduce 98.96 barn.
b: Results for $^{238}U(n,\gamma)^{239}U$ compared to spectrum-averaged values obtained with the data from libraries. A 3% normalization was applied to IRMM-a and IRMM-b data.

			$^{235}U(n,\gamma)$ cross section (barn)					
Sample	Neutron energy	$^{236}U/^{235}U$ ratios (in units of 10^{-9})	This work	ENDF/ B-VII.1	JENDL -4.0	CENDL -3.1	RUSFOND 2010	JEFF -3.1.2
IRMM-3	Thermal	7.11 ± 0.21	99.5 ± 2	98.96	98.71	98.96	98.96	98.96
IRMM-5	Thermal	28.2 ± 0.5	101.5 ± 2					
IRMM-a	$kT \sim 25$ keV	1.061 ± 0.045	0.651 ± 0.036	0.679	0.685	0.681	0.679	0.681
IRMM-b	426 keV	0.713 ± 0.026	0.169 ± 0.008	0.186	0.196	0.169	0.186	0.186

			$^{238}U(n,\gamma)$ cross section (barn)					
Sample	Neutron energy	$^{239}U/^{238}U$ ratios (in units of 10^{-10})	This work	ENDF/ B-VII.1	JENDL -4.0	CENDL -3.1	RUSFOND 2010	JEFF -3.1.2
IRMM-3	Thermal	1.97 ± 0.04	2.75 ± 0.04	2.68	2.68	2.68	2.68	2.68
IRMM-5	Thermal	7.76 ± 0.16	2.79 ± 0.04					
IRMM-a	$kT \sim 25$ keV	6.37 ± 0.20	0.391 ± 0.017	0.409	0.407	0.407	0.409	0.405
IRMM-b	426 keV	4.58 ± 0.11	0.108 ± 0.004	0.109	0.110	0.109	0.109	0.116

5^+ with a particle energy of ~17.8 MeV were selected in a subsequent analyzing magnet.

The ^{235}U and ^{238}U beam intensity was measured as particle current collected in a Faraday cup. The low-intensity ^{236}U and ^{233}U (or ^{239}Pu and ^{242}Pu) beam was passing another electrostatic and magnetic deflector for further filtering from unwanted background ions, and was finally counted in a TOF detector and an ionization chamber. The TOF signals added information of isotopic background to identify residual particles, e.g., spurious ^{235}U and ^{238}U. The ionization chamber was used to separate particles of identical magnetic and electrostatic rigidity but of different energies. VERA represents one of the most sensitive facilities for such experiments and is routinely used for actinide measurements [13,17,32].

The uranium isotopes were measured by an automated procedure, switching alternatively between $^{235,238}U$ current measurement and rare isotope ($^{233,236}U$) counting to calculate $^{236}U/^{233}U$, $^{236}U/^{238}U$, and $^{233}U/^{238}U$ ratios. In addition, the $^{233}U/^{238}U$ atom ratio was controlled by the ^{233}U spike. All samples prepared from the keV irradiations were compared to identical nonirradiated blank samples and to the two reference pellets from the BNC irradiations. The $^{236}U/^{238}U$ (and $^{233}U/^{238}U$) isotope ratio in the nonirradiated samples was measured precisely from ~60 sputter samples (i.e., for about twice the number of irradiated sputter samples, thus accounting for >50% of the total measuring time) to verify the natural ^{236}U content (contribution ~1%–2% to the final uncertainty, Fig. 3, Supplemental Material, Table T1 [11]).

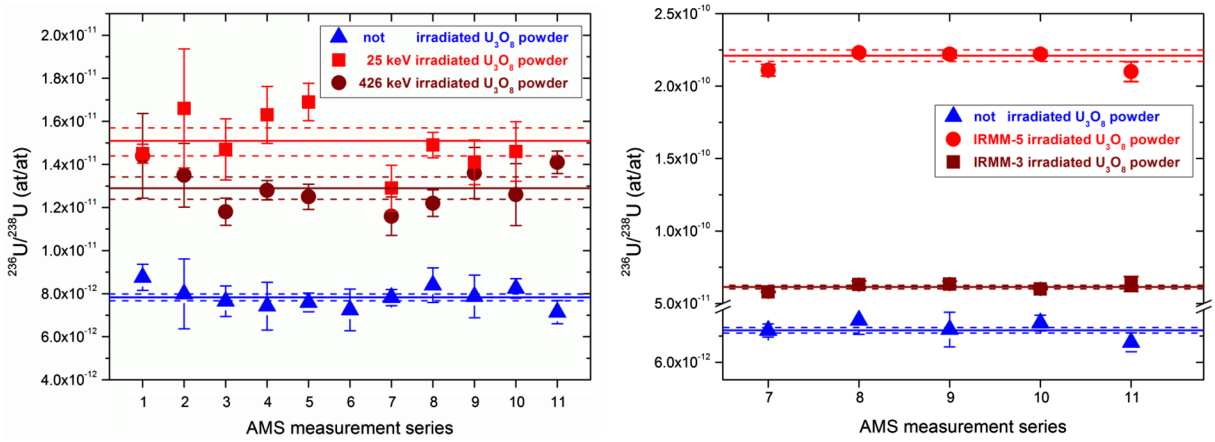

FIG. 3 (color online). $^{236}U/^{238}U$ isotope ratios as measured with AMS at VERA. Left: mean isotope ratios obtained for the two samples irradiated at KIT and a nonirradiated blank. Right: samples irradiated at BNC; note the higher ratios due to the 150–600 times higher thermal capture cross section. These samples visualize the reproducibility of the AMS method (±1.5%).

TABLE III. Spectrum-averaged cross-section ratios obtained in this work and compared to evaluated data.

		This work	ENDF/B-VII.1	JENDL-4.0	CENDL-3.1	RUSFOND2010	JEFF-3.1.2
$\sigma_{238U(n,\gamma)}/\sigma_{235U(n,\gamma)}$	25 keV	0.60 ± 0.03	0.59	0.56	0.60	0.59	0.59
	426 keV	0.64 ± 0.03	0.59	0.56	0.64	0.59	0.62
		This work	ENDF/B-VII.1		Standards-eval. [30]		
$\sigma_{238U(n,\gamma)}/\sigma_{197Au(n,\gamma)}$	25 keV	0.63 ± 0.03	0.66		0.67		
	426 keV	0.68 ± 0.03	0.69		0.69		

Similar to the ^{236}U and ^{233}U measurements, the ^{239}Pu atoms were counted together with the ^{242}Pu spike. Altogether, 11 series of AMS measurements were performed for $^{235}\mathrm{U}(n,\gamma)$ and five series for $^{238}\mathrm{U}(n,\gamma)$. Particular attention was paid to quantify and minimize systematic uncertainties in AMS: ^{236}U was measured relative to ^{238}U, but also relative to the ^{233}U spike, which was counted in the same way as ^{236}U. Using a set of in-house ^{236}U standards (ViennaKkU, [13]) the $^{236}\mathrm{U}/^{238}\mathrm{U}$ data could be reproduced within 1.5% and statistical uncertainties were <1%. The mean $^{236}\mathrm{U}/^{238}\mathrm{U}$ isotope ratios are plotted in Fig. 3 for the samples irradiated at KIT (left) and BNC (right).

Averaging all data, we obtained a 1.5% systematic offset between the results when based on the $^{236}\mathrm{U}/^{233}\mathrm{U}$ or the $^{236}\mathrm{U}/^{238}\mathrm{U}$ ratios. Using the $^{236}\mathrm{U}/^{233}\mathrm{U}$ ratios, we calculate a thermal $^{235}\mathrm{U}(n,\gamma)$ cross section of 99.5 and 101.5 barn for the two samples. Renormalizing the mean value of 100.5 ± 2.1 barn to the recommended value of 98.96 barn [4–8] yields a scaling factor of 1.6%, which was then applied to the results of the KIT irradiations. Similarly, we obtained thermal $^{238}\mathrm{U}(n,\gamma)$ cross sections of 2.75 and 2.79 barn from the $^{239}\mathrm{Pu}/^{242}\mathrm{Pu}$ AMS ratios, the average 3% higher than the recommended value of 2.68 barn. This absolute normalization was again applied to the KIT samples for $^{238}\mathrm{U}(n,\gamma)$.

The final uncertainties for the spectrum-averaged cross sections of ^{235}U and ^{238}U in this work were ~5% and ~4% for $kT \sim 25$ and 426 keV, respectively. Compared to data libraries (Table II) the SACS of ^{235}U and ^{238}U for $kT \sim 25$ keV were found to be generally ~4% lower. For the broad energy distribution at 426 keV, $^{235}\mathrm{U}(n,\gamma)$ agrees with CENDL, is 16% lower than JENDL, and 9% lower than ENDF, RUSFOND, and JEFF. $^{238}\mathrm{U}(n,\gamma)$ for 426 keV agrees with all data libraries within ~1%, except JEFF which is 7% (~2σ) higher. We note, in all cases we used the $^{197}\mathrm{Au}(n,\gamma)$-ENDF/B-VII.1 cross sections for the neutron fluence determination. If we apply the Au value used in nuclear astrophysics applications for the 25-keV spectrum (adjusted for our geometry), our (n,γ) values for ^{235}U and ^{238}U become lower by 4.6%, resulting in a 1.5σ difference to ENDF for both isotopes for $kT \sim 25$ keV.

Because we measured both (n,γ) cross sections in the same samples, we can compare the measured isotope ratios directly with the cross-section ratios [Eq. (2)]; i.e., any uncertainty from the neutron fluence vanishes. We obtain a spectrum-averaged cross-section ratio $\sigma_{238U(n,\gamma)}/\sigma_{235U(n,\gamma)}$ of 0.60 ± 0.03 for $kT \sim 25$ keV, in agreement with the ENDF, JEFF, and RUSFOND ratio of 0.59, JENDL (0.56) and CENDL (0.60) (Tab. III). Similarly, we obtain an experimental value of 0.64 ± 0.03 for 426 keV, compared to the ENDF-ratio (0.59), JENDL (0.56), and in good agreement with JEFF (0.62) and CENDL (0.64). Thus, we can investigate the discrepancies observed in $^{235}\mathrm{U}(n,\gamma)$ at keV energies by normalizing our AMS ratios with the well-known ^{238}U capture values from data libraries. With the ^{238}U data from ENDF-B/VII.1 we calculate a ^{235}U cross section for $kT \sim 25$ keV of 681 ± 27 mbarn, close to the 679 mbarn calculated from ENDF-B/VII.1. Analogously, for 426 keV our normalized value for $^{235}\mathrm{U}(n,\gamma)$ becomes 171 ± 6 mbarn, 8% (2σ) lower than the ENDF value (186 mbarn). Similar results are obtained for JENDL, CENDL, and RUSFOND, but the JEFF ^{238}U-data yields ^{235}U cross sections in perfect agreement (2% and 1% difference for 25 and 426 keV). Further, our SACS ratio $\sigma_{238U}/\sigma_{197Au}$ for 426 keV is in agreement with ENDF and the standards evaluation [30], but for $kT = 25$ keV our value is ~5% lower (with ~5% uncertainty). This difference would be fully compensated by the Au value used in nuclear astrophysics applications [27], however, with the consequence of lower absolute values for ^{235,238}U neutron capture in this energy range (see above). Recent experimental work on $\mathrm{Au}(n,\gamma)$ in this energy region at n_TOF [33] and IRMM [34] do agree with ENDF (and the standards cross section) within their uncertainty of 3.6% and 2.7%. We further note that a high-accuracy gold-capture measurement was just recently performed at IRMM/GELINA [35]. We conclude our $^{238}\mathrm{U}(n,\gamma)$ cross-section data at $kT = 25$ keV and the recent direct $\mathrm{Au}(n,\gamma)$ measurements favor a higher gold cross-section value than used by the astrophysics community. Thus, any additional support from an accurate $\mathrm{Au}(n,\gamma)$ measurement will be very valuable.

In summary, we have applied a new and completely independent method for a simultaneous measurement of ^{235}U and ^{238}U neutron-capture cross sections using milligram-sized samples. Atom ratios were measured via accelerator mass spectrometry with a precision of 2%–4%, completely unaffected from any fission and other γ-ray background. Our spectrum-averaged $^{235}\mathrm{U}(n,\gamma)$ cross section for $kT \sim 25$ keV of 651 ± 36 mbarn is lower, though

compatible with the recent Los Alamos data of 700 ± 60 mbarn [1]. Our ^{235}U and ^{238}U data at keV neutron energies will serve as anchor points for complementary TOF measurements. We have utilized this combination of activation and AMS in a series of capture measurements using the same irradiation geometry, and in additional activations within the European EUFRAT and ERINDA programme [36]. In the future, new powerful irradiation facilities, e.g., FRANZ [28,37] and SARAF [38], will provide new opportunities for such measurements, which might allow μg-sized samples.

We would like to thank S. Richter (IRMM, Geel, Belgium) for providing the natural uranium material with low ^{236}U content (BC0206-1) used in this work. We acknowledge support from the European EFNUDAT programme (FP6-036434), from the IAEA (No. 14336/R0, CRP MANREAD), from NAP VENEUS OMFB 00184/2006 and from the Austrian Science Fund, Projects No. AP20434, No. AI00428, and No. J3503.

[†]Present address: School of Physics and Astronomy, University of Edinburgh, Edinburgh EH9 3JZ, United Kingdom.
[‡]Present address: Institute for Nuclear Waste Disposal, Karlsruhe Institute of Technology (KIT), Campus North, 76021 Karlsruhe, Germany.
[*]Corresponding author.
anton.wallner@anu.edu.au

[1] M. Jandel *et al.*, Phys. Rev. Lett. **109**, 202506 (2012).
[2] C. Guerrero *et al.* (n_TOF Collaboration), Eur. Phys. J. A **48**, 29 (2012).
[3] M. Heil, R. Reifarth, M. M. Fowler, R. C. Haight, F. Käppeler, R. S. Rundberg, E. H. Seabury, J. L. Ullmann, J. B. Wilhelmy, and K. Wisshak, Nucl. Instrum. Methods Phys. Res., Sect. A **459**, 229 (2001).
[4] M. B. Chadwick *et al.*, Nucl. Data Sheets **112**, 2887 (2011).
[5] K. Shibata *et al.*, J. Nucl. Sci. Technol. **48**, 1 (2011).
[6] A. J. Koning *et al.*, J. Korean Phys. Soc. **59**, 1057 (2011); http://www.oecd-nea.org/dbforms/data/eva/evatapes/jeff_31/JEFF312/.
[7] S. V. Zabrodskaya *et al.*, VANT, Nuclear Constants **1**–**2**, 3 (2007); http://www.ippe.ru/podr/abbn/libr/rosfond.php.
[8] Z. G. Ge *et al.*, J. Korean Phys. Soc. **59**, 1052 (2011).
[9] http://www.nea.fr/dbdata/hprl/.
[10] Exfor database. https://www-nds.iaea.org/exfor/exfor.htm.
[11] See Supplemental Material at http://link.aps.org/supplemental/10.1103/PhysRevLett.112.192501 for details on the AMS measurements, on the uncertainty budget and a list of existing experimental data.
[12] F. Corvi, L. Calabretta, M. Merla, M. S. Moore, and T. Van Der Veen, Report from CEC-Countries and CEC to NEANDC, Report No. 232, 1982.
[13] P. Steier *et al.*, Nucl. Instrum. Methods Phys. Res., Sect. B **268**, 1045 (2010); **294**, 160 (2013).
[14] X.-L. Zhao, M.-L. Nadeau, L. R. Kilius, and A. E. Litherland, Nucl. Instrum. Methods Phys. Res., Sect. B **117**, 249 (1996).
[15] L. K. Fifield, Quaternary Geochronology **3**, 276 (2008).
[16] D. Berkovits, H. Feldstein, S. Ghelberg, A. Hershkowitz, E. Navon, and M. Paul, Nucl. Instrum. Methods Phys. Res., Sect. B **172**, 372 (2000).
[17] A. Wallner, K. Buczak, F. Quinto, P. Steier, T. Belgya, L. Szentmiklosi, M. Bichler, I. Dillmann, F. Käppeler, and A. Mengoni, J. Korean Phys. Soc. **59**, 1410 (2011).
[18] X. Wang, S. Jiang, M. He, K. Dong, C. Xiao, Y. Hu, Q. You, H. Chen, L. Hou, W. Yu, and X. Ruan Phys. Rev. C **87**, 014612 (2013).
[19] H. Nassar *et al.*, Phys. Rev. Lett. **94**, 092504 (2005).
[20] I. Dillmann *et al.*, Phys. Rev. C **79**, 065805 (2009).
[21] G. Rugel, I. Dillmann, T. Faestermann, M. Heil, F. Käppeler, K. Knie, G. Korschinek, W. Kutschera, M. Poutivtsev, and A. Wallner, Nucl. Instrum. Methods Phys. Res., Sect. B **259**, 683 (2007).
[22] A. Wallner, Nucl. Instrum. Methods Phys. Res., Sect. B **268** 1277 (2010); A. Wallner *et al.*, Pub. Astron. Soc. Aust. **29**, 115 (2012).
[23] A. Verbruggen *et al.*, Report EUR 22924 EN, Belgium, 2007.
[24] H. Beer and F. Käppeler, Phys. Rev. C **21**, 534 (1980).
[25] T. Belgya, Phys. Procedia **31**, 99 (2012).
[26] L. Szentmiklósi, T. Belgya, Zs. Révay, and Z. Kis, J. Radioanal. Nucl. Chem. **5286**, 505 (2010); Budapest Neutron Centre: http://www.bnc.hu.
[27] W. Ratynski and F. Käppeler, Phys. Rev. C **37**, 595 (1988).
[28] F. Käppeler, R. Gallino, S. Bisterzo, and W. Aoki, Rev. Mod. Phys. **83**, 157 (2011).
[29] R. Reifarth, M. Heil, F. Käppeler, and R. Plag, Nucl. Instrum. Methods Phys. Res., Sect. A **608**, 139 (2009).
[30] A. D. Carlson *et al.*, Nucl. Data Sheets **100**, 3215 (2009); (2014) (to be published).
[31] http://irmm.jrc.ec.europa.eu/reference_materials_catalogue/catalogue/IRMM/Pages/index.aspx.
[32] A. Wallner *et al.*, Eur. Phys. J. Web Conf. **35**, 01003 (2012).
[33] C. Lederer *et al.*, Phys. Rev. C **83**, 034608 (2011).
[34] G. Feinberg *et al.*, Phys. Rev. C **85**, 055810 (2012).
[35] C. Massimi *et al.* (to be published).
[36] http://irmm.jrc.ec.europa.eu/activities/eufrat/; http://www.erinda.org/, (to be published).
[37] U. Ratzinger *et al.*, in *Proceedings of IPAC'10, Kyoto, Japan, 2010*, http://accelconf.web.cern.ch/AccelConf/IPAC10/index.htm.
[38] L. Weissman *et al.*, in *Proceedings of Linac, Tsukuba, 2010*, http://accelconf.web.cern.ch/AccelConf/LINAC2010/html/sessi0n.htm.